

# Surface-restricted effective interactions in a shell model application to $^{88}\text{Sr}$ †

N. Auerbach

*Department of Physics and Astronomy, Tel-Aviv University, Tel-Aviv, Israel\**  
*and Brookhaven National Laboratory, Upton, New York 11973*

J. P. Vary

*Ames Laboratory-ERDA and Department of Physics, † Iowa State University, Ames, Iowa 50011*  
*and Brookhaven National Laboratory, Upton, New York 11973*

(Received 3 November 1975)

We compare conventional phenomenological effective interactions acting throughout the nuclear volume with some surface restricted effective interactions for the particle-hole spectrum and properties of  $^{88}\text{Sr}$  in a basis of neutron and proton orbitals. The surface restricted forces produce greater configuration mixing and enhance the neutron particle-hole contributions to the lowest-lying states and thus result in better agreement with experiment.

NUCLEAR STRUCTURE  $^{88}\text{Sr}$ , Surface or density dependent effective interactions, particle-hole shell model structure, calculated levels,  $J$ ,  $\pi$ ,  $B(\Lambda)$  spectroscopic factors.

## I. INTRODUCTION

There has been considerable interest in the density dependence of the effective interaction for both Hartree-Fock and shell model applications.<sup>1-17</sup> In early discussions the field was stimulated by qualitative arguments within the spirit of a local density approximation. It was reasoned that nucleons interacting on the surface of the nucleus, do not have their available phase space for scattering hindered by the Pauli principle as much as those in the interior. In more recent detailed microscopic Hartree-Fock calculations<sup>13-17</sup> the density dependence of the effective interaction has played an important role in achieving quantitative agreement between theory and experiment for the ground state binding energies and density distributions of a few nuclei.

The use of density dependence in phenomenological effective shell model interactions has recently been considered by Sharp and Zamick<sup>3</sup> who employed the Skyrme force<sup>5</sup> with the parameters found successful in Hartree-Fock<sup>14</sup> calculations. However, the work of Negele and Vautherin<sup>16</sup> raises some question of the suitability of this particular parametrization for shell model purposes.<sup>18</sup> In addition, Ring and Speth<sup>4</sup> have fitted parameters of a Migdal<sup>10</sup> type force to the  $^{208}\text{Pb}$  region isotope shifts and to the level properties of  $^{208}\text{Pb}$  in a large space random phase approximation (RPA) calculation.

It is the purpose of this work to introduce some simple phenomenological forms of density dependent effective shell model interactions and examine their qualitative effects compared with some

simple standard interactions acting throughout the nuclear volume. For this purpose we select  $^{88}\text{Sr}$ , which has been rather well studied experimentally, in order to present the results for a few conventional and a few surface restricted effective interactions.

## II. SHORT REVIEW OF $^{88}\text{Sr}$

With  $N=50$  and  $Z=38$ ,  $^{88}\text{Sr}$  might be expected to exhibit a nearly pure low-lying proton spectrum. However,  $(d, p)$ <sup>19,20</sup> and  $(p, p')$ <sup>21-23</sup> experiments and analyses have indicated significant contributions to the low-lying  $^{88}\text{Sr}$  states from neutron 1p-1h configurations. For example, the  $(d, p)$  experiment indicates that the  $|g_{9/2}^{-1}d_{5/2}\rangle$  neutron configuration in the  $J=2^+$  (1.8 MeV) state is about 25%. It is worth noting that the second  $2^+$  at 3.22 MeV exhibits no contribution from states with a  $g_{9/2}$  neutron hole in the  $(d, p)$  experiments. This is verified in the  $(\eta, \gamma)$  experiments<sup>24</sup> by the lack of a direct transition to the 3.22 MeV state from the capture state. Since the  $|g_{9/2}^{-1}d_{5/2}\rangle$  single-particle plus single-hole energy is greater than 4 MeV, it indicates that residual neutron particle-hole interactions play an important role in the properties of these states.

The collective nature of the lowest  $2^+$  and  $3^-$  is demonstrated by the large  $B(E2)$  and  $B(E3)$  values measured for these states. This fact and the neutron admixture problem together provide some interesting tests of the various residual interactions used in the present calculations.

The  $^{89}\text{Y}(d, ^3\text{He})^{88}\text{Sr}$  studies<sup>25,26</sup> indicate the presence of low-lying unnatural parity  $1^+$  and  $3^+$  states

at 3.48 and 3.64 MeV, respectively. Further spectroscopic information on these and other low-lying states is obtained in this reaction. Earlier  $\beta$  decay studies of  $^{86}\text{Rb}$  (Ref. 27) as well as more recent<sup>28</sup> studies give much additional information on the wave functions of the lower spin states especially. Most recently, the reaction  $^{86}\text{Kr}(d, 2n)^{88}\text{Sr}$  has found<sup>29</sup> new states of high spin in the 3.5 to 4.5 MeV range of excitation energy which provide tests for the choice of model space.

Several previous calculations have dealt with the spectrum and properties of  $^{88}\text{Sr}$ .<sup>23,30-35</sup> Shastri<sup>31</sup> has reported a 1p-1h calculation with both neutrons and protons of only the  $2^+$  and  $3^-$  levels of  $^{88}\text{Sr}$  in which he included all unperturbed 1p-1h configurations up to 8 MeV, and some of the 1p-1h configurations up to 16 MeV. The residual interaction employed was a Gaussian with a Rosenfeld admixture.<sup>37</sup>

A different approach was taken by Hughes<sup>32</sup> in a study of only the positive parity states in  $^{88}\text{Sr}$ . The  $^{90}\text{Zr}$  nucleus was chosen as the inert core, and the  $^{88}\text{Sr}$  spectrum was described in terms of two independent spectra. The first spectrum included two proton holes in the  $p_{1/2}$ ,  $p_{3/2}$ ,  $f_{5/2}$ , and  $f_{7/2}$  orbits. The second treated protons as inert and studied a neutron in the  $d_{5/2}$ ,  $s_{1/2}$ ,  $d_{3/2}$ , and  $g_{7/2}$  particle orbits coupled with a neutron hole in the  $g_{9/2}$  orbit. Thus, Hughes did not allow the neutrons to interact with the protons.

The lowest  $1^+$  state was treated by Cecil, Kuo, and Tsai<sup>35</sup> in studying the mixing with the giant magnetic dipole state. They used a realistic interaction in a large space RPA calculation. This effort was extended by Cecil, Chestnut, and McGrath<sup>23</sup> to the lowest-lying  $3^+$  state in an experimental and theoretical study of  $(p, p')$  to these two states.

Other RPA studies<sup>33,21</sup> of only the first  $2^+$ ,  $3^-$ , and  $4^+$  states have been performed in the past using phenomenological forces with a major emphasis on reproducing the collective transition strengths.

The present study includes a sizable p-h model space for both neutrons and protons which are allowed to interact and we report all states of both spins and parities that are calculated up to 5 MeV of excitation energy in  $^{88}\text{Sr}$ . One advantage over previous calculations, for example, is that this model space yields  $5^-$ ,  $6^-$ , and  $7^-$  states in the region where they are believed to be observed by Arnell, Nilsson, and Stankiewicz.<sup>29</sup>

### III. CONFIGURATIONS, SINGLE-PARTICLE, AND SINGLE-HOLE ENERGIES

By considering the unperturbed energies of the 2p-2h configurations one can estimate a suitable

choice of neutron and proton orbitals to be included in a 1p-1h calculation. The lowest unperturbed 2p-2h configurations,  $|p_{3/2}^{-2}p_{1/2}^2\rangle$  and  $|f_{5/2}^{-1}p_{3/2}^{-1}p_{1/2}^2\rangle$  occur between 6 and 7.5 MeV. The lowest unperturbed 2p-2h configuration of negative parity is  $|p_{3/2}^{-2}p_{1/2}g_{9/2}\rangle$  and occurs around 8 MeV. One can hope, therefore, that the low-lying levels can be adequately described by a 1p-1h calculation which includes unperturbed configurations up to  $\sim 7$  MeV.

In all the calculations reported here, we include all the low-lying neutron and proton 1p-1h configurations arising from the proton states  $p_{1/2}$ ,  $g_{9/2}$ ,  $f_{5/2}^{-1}$ , and  $p_{3/2}^{-1}$  and from the neutron states  $d_{5/2}$ ,  $s_{1/2}$ ,  $d_{3/2}$ ,  $g_{7/2}$ ,  $p_{1/2}^{-1}$ , and  $g_{9/2}^{-1}$ . (See Fig. 1.) This space yields states from  $J=0$  through  $J=7$  and states of both parities.

The single-particle energies  $C_{i_j}$  and the single-hole energies  $B_{i_j}$  were taken from the known binding energies,<sup>36</sup> the single-particle levels, and the single-hole levels of neighboring nuclei. The  $^{88}\text{Sr}$  ground state was taken as the zero energy reference. For the protons we get in MeV:

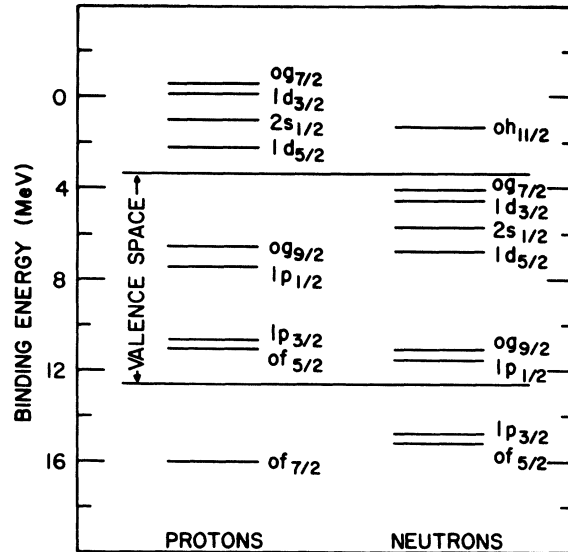


FIG. 1. Shell model single-particle orbitals as a function of their binding energy in the vicinity of the Fermi surface in  $^{88}\text{Sr}$ . The orbitals between the two heavy horizontal bars are included in the particle-hole shell model calculations described in the text. The binding energy of the proton orbitals above the valence space are not well known, so they are approximated as given by the known neutron spacings. In an analogous fashion we estimate the two neutron orbitals below the valence space. The  $0f_{7/2}$  proton and the  $0h_{11/2}$  neutron orbitals are crudely estimated from knowing their positions in other regions of the Periodic Table. All orbitals below and including the  $1p_{3/2}$  proton and  $0g_{9/2}$  neutron are assumed occupied in the ground state of  $^{88}\text{Sr}$ .

$$C_{p_{1/2}} = \text{BE}^{(89\text{Y})} - \text{BE}^{(88\text{Sr})} = -7.46$$

$$C_{s_{9/2}} = C_{p_{1/2}} + 0.91 = -6.55$$

$$B_{p_{3/2}} = \text{BE}^{(87\text{Rb})} - \text{BE}^{(88\text{Sr})} = 10.61$$

$$B_{f_{5/2}} = B_{p_{3/2}} + 0.40 = 11.01$$

and for the neutrons:

$$C_{d_{5/2}} = \text{BE}^{(89\text{Sr})} - \text{BE}^{(88\text{Sr})} = -6.77$$

$$C_{s_{1/2}} = C_{d_{5/2}} + 1.05 = -5.72$$

$$C_{d_{3/2}} = C_{d_{5/2}} + 2.20 = -4.57$$

$$C_{s_{7/2}} = C_{d_{5/2}} + 2.70 = -4.07$$

$$B_{s_{9/2}} = \text{BE}^{(87\text{Sr})} - \text{BE}^{(88\text{Sr})} = 11.12$$

$$B_{p_{1/2}} = B_{s_{9/2}} + 0.388 = 11.51$$

#### IV. RESIDUAL INTERACTIONS

Six calculations are reported here, each using a different residual interaction. The first three cases are frequently used central interactions, with appropriate exchange admixtures, which act throughout the nuclear volume. The other three are restricted to the nuclear surface. With some important exceptions the results of the first three cases are similar as are the results of the last three. However, the results of the surface interactions differ sharply from those of the first three. In all cases, except case (4), where it does not apply,  $\hbar\omega$ , the oscillator energy, was chosen to be 10 MeV.

*Case (1).* A Gaussian shape with Rosenfeld admixture<sup>37</sup> was chosen with parameters:  $V_0 = -40$  MeV and  $r_0 = 1.85$  fm. This interaction was found by Shastry<sup>31</sup> to work well in his large space calculations of selected  $2^+$  and  $3^-$  states.

*Case (2).* A Yukawa interaction also with Rosenfeld<sup>37</sup> admixture with:  $V_0 = -50$  MeV and  $r_0 = 1.37$  fm. The results found in case (2) were nearly identical with those of case (1).

*Case (3).* The Kallio-Kolltveit<sup>38</sup> (KK) potential was used in relative even states with the radial integrals evaluated using the Moszkowski-Scott separation method<sup>39</sup> to see if a more "realistic" interaction could improve the low-lying spectrum. The results show that the KK potential produces a low-lying spectrum quite similar to cases (1) and (2).

*Case (4).* All the above residual interactions have been employed widely in the past. An interaction of a different type is the surface  $\delta$  Interaction<sup>2,17,40</sup> (SDI) in which the particles interact only when they are at the surface of the nucleus, and then only by means of a zero-range interaction:

$$V(\vec{r}_i, \vec{r}_j) = -g\delta(r_i - R_0)\delta(r_j - R_0)\delta(\Omega_{ij}), \quad (1)$$

where  $R_0$  is the nuclear radius,  $r_i$  and  $r_j$  are the nucleon coordinates, and  $\Omega_{ij}$  is the angle between the two nucleons. The additional assumption of equal single-particle radial wave functions at the surface permits the SDI to be written

$$V_{ij} = -4\pi G\delta(\Omega_{ij}) \quad (2)$$

in which the strength  $G$  is the only adjustable parameter. This form of the SDI has been employed in calculations by some investigators<sup>40,41</sup> where we cite only the earliest applications. Mathematical simplicity is a strong advantage of this form, since it leads to a particularly simple equation for the two-particle matrix element. This is the form we employ here.

Since the present calculations involve the proton-neutron interaction we need both  $T=0$  and  $T=1$  matrix elements. Following previous work<sup>42</sup> we calculate these matrix elements by selecting two different values of  $G$  for the two different isospin states. The values of  $G_T$  used in the present work were  $G_1 = 0.7$  and  $G_0 = 0.9$  which are approximately consistent with those of Ref. 42. We did not perform a careful search, since these were observed to produce reasonable agreement with the experimental energy levels.

Another form equivalent to that in Eq. (1) is

$$V(\vec{r}_i, \vec{r}_j) = -g'\delta(r_{ij})\delta(R_{ij} - R_0), \quad (3)$$

where  $r_{ij}$  is the relative coordinate and  $R_{ij}$  is the center of mass coordinate in the interacting nucleons.

*Case (5).* It is possible to relax some of the restrictive features of the SDI but at the price of increased mathematical complexity. For example, one can replace  $\delta(r_{ij})$  in Eq. (3) by a finite-range interaction such as one of those previously mentioned, or replace the  $\delta(R_{ij} - R_0)$  by a weighting function which peaks at the nuclear surface. The latter case would be in the spirit of the modified  $\delta$  interaction (MDI).<sup>2,17</sup> One could perform both replacements and forego the assumption of equal single-particle radial wave functions. In general, this procedure would lead to an interaction of the form:

$$V(\vec{r}_i, \vec{r}_j) = v(r_{ij})F(R_{ij}). \quad (4)$$

This is more general than the customary central residual interaction and it allows for certain forms of density dependence of the effective nuclear force. Other forms have been employed in Hartree-Fock calculations, but they cannot be written so simply as Eq. (4) in the relative center of mass variables. Wong and Moszkowski<sup>43</sup> have shown that the above choice, as well as two others they

studied, is adequate for parametrizing density dependence for Hartree-Fock applications. Under certain conditions, they seem to find that the form (4) is to be preferred.

For the Brandow<sup>44</sup> linked cluster theory of the effective shell model interaction the choice of passive core particle space and active valence orbitals affects the density dependence of the effective interaction even in lowest order, because it defines the Pauli operator in the Bethe-Goldstone equation. In shell model calculations, one often wishes to see the effect on the fitted residual interaction of varying the choice of Hilbert spaces. Allowing  $F(R_{ij})$  to vary with different choices of spaces while keeping  $v(r_{ij})$  fixed offers a possibly appealing way to consider such effects. The method of calculation outlined below is economically feasible for pursuing such studies.

For case (5) we chose the residual interaction of case (2) for  $v(r_{ij})$ .  $F(R_{ij})$  was taken to be

$$F(R_{ij}) = A_0 \delta(R_{ij} - R_0) \quad (5)$$

with  $R_0 = 5.35$  fm. Several values of  $A_0$  were tried.  $A_0 = 5.5$  provided an acceptable fit to the observed spectrum.

Case (6). The pervading philosophy of being able to treat residual interactions of the type in Eq. (4) should be eventually to incorporate realistic two-

body interactions in an appropriate way. With this in mind we chose  $v(r_{ij})$  to be the Kallio-Kolltveit potential [case (3)] and keep the same  $F(R_{ij})$  given in Eq. (5). Here  $A_0 = 5.0$  was found to give a satisfactory fit to the data.

## V. METHOD

Each two-body matrix element with antisymmetrized and normalized two-particle states  $|abJT\rangle$  for an interaction of type (4) when only central forces are considered can be expressed in the simple form:

$$\langle abJT|V|cdJT\rangle = \sum_i J_i \sum_{jS} I_j^S \epsilon_{ij}^S(abcdJT), \quad (6)$$

where the  $I_j$  and the  $J_i$  are the Talmi integrals<sup>45</sup> for the relative and the center of mass coordinates, respectively, and the  $\epsilon$ 's are interaction independent constants, and  $S$  represents the total spin of the two nucleons. If we represent the oscillator radial wave function by  $R_{nl}(r)/r$ , then

$$I_j = \int_0^\infty R_{0j}^2(r) v(r) dr, \quad (7)$$

$$J_i = \int_0^\infty R_{0i}^2(R) F(R) dr, \quad (8)$$

$$\begin{aligned} \epsilon_{ij}^S(abcdJT) = & 2 \left[ \frac{[j_a][j_b][j_c][j_d]}{(1+\delta_{ab})(1+\delta_{cd})} \right]^{1/2} \sum_L [S][L] \left[ \frac{1 - (-1)^{S+T+L}}{2} \right] \begin{Bmatrix} l_a & \frac{1}{2} & j_a \\ l_b & \frac{1}{2} & j_b \\ L & S & J \end{Bmatrix} \begin{Bmatrix} l_c & \frac{1}{2} & j_c \\ l_d & \frac{1}{2} & j_d \\ L & S & J \end{Bmatrix} \\ & \times \sum_{N\Lambda} \alpha_i^{NN'\Lambda} \sum_{\nu\lambda} \alpha_j^{\nu\lambda} \langle \nu\lambda N\Lambda, L | n_a l_a n_b l_b, L \rangle \langle \nu\lambda N'\Lambda, L | n_c l_c n_d l_d, L \rangle \end{aligned} \quad (9)$$

with  $[S] = 2S + 1$ , and, in which, with  $p = j - l$

$$\begin{aligned} \alpha_j^{nn'l} = & (-1)^p [2(l+p) + 1]! \left[ \frac{(2l+2n+1)!(2l+2n'+1)!}{2^{n+n'} n! n'!} \right]^{1/2} \\ & \sum_{k=\max(0, p-n')}^{\min(n, p)} \binom{n}{k} \binom{n'}{p-k} \frac{1}{(2l+2k+1)!(2l+2p-2k+1)!}. \end{aligned} \quad (10)$$

The curly bracketed quantities are the 9- $j$  coefficients for the transformation from the  $L$ - $S$  to the  $j$ - $j$  representation. The  $\nu\lambda$  and  $N\Lambda$  are the relative and center of mass quantum numbers, respectively, and the bracket  $\langle \nu\lambda N\Lambda, L | n_a l_a n_b l_b, L \rangle$  is the standard Brody-Moshinsky transformation bracket.<sup>46</sup> The  $\alpha$ 's are defined by the equation

$$\begin{aligned} & \int_0^\infty R_{nl}(r) v(r) R_{n'l}(r) dr \\ & = \sum_j \alpha_j^{nn'l} \int_0^\infty R_{0j}(r) v(r) R_{0j}(r) dr \\ & = \sum_j \alpha_j^{nn'l} I_j. \end{aligned} \quad (11)$$

## VI. RESULTS

Of the states calculated we report only those below 5 MeV for the six cases described above. In addition, we present selected wave functions, transition probabilities, and spectroscopic factors—where these quantities can be compared with experimental data.

Figure 2 illustrates the experimental and calculated spectra. The results appear to cluster together depending chiefly on whether the interactions work throughout the nuclear volume [cases (1)–(3)] or whether they act only at the surface [cases (4)–(6)].

The following comment should be made. In a separate calculation we found that a very sub-

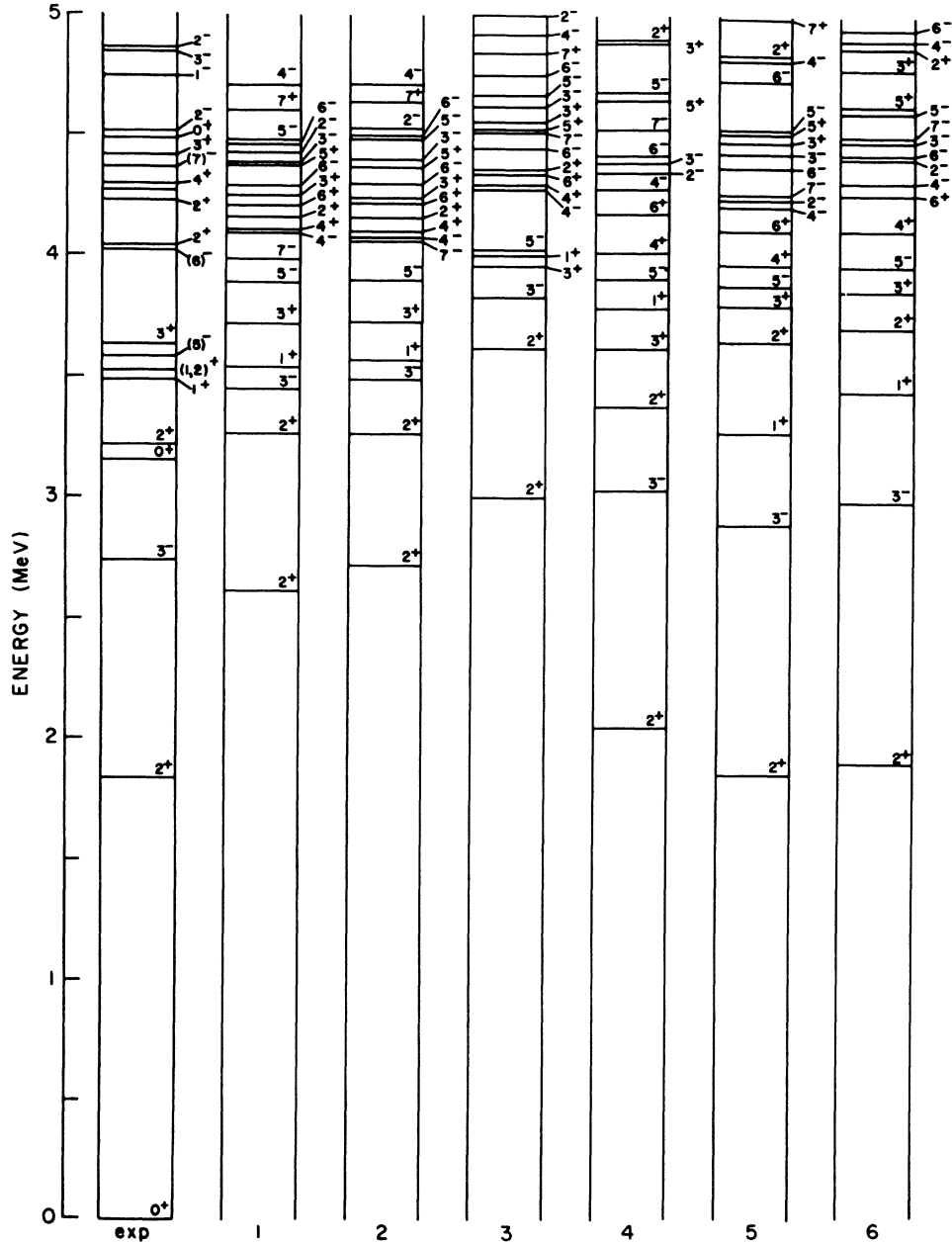


FIG. 2. Experimental and particle-hole shell model spectra for  $^{88}\text{Sr}$ . The experimental spectra is our best estimate based on the experiments cited in the text. No excited  $0^+$  states can be constructed in the 1p-1h model space so that no comparison with the 3.15 or 4.484 MeV states is possible. The columns of theoretical results labeled 1 through 6 correspond to effective interactions cases (1) through (6) described in the text. All states obtained below 5 MeV of excitation are displayed.

stantial increase in the strength of the two-body interaction in cases (1)–(3) generally improves the energies of the lowest states but does not significantly increase the configuration mixing. Nevertheless, one can ask the question whether the value  $A_0$  obtained for cases (5) and (6) disguises an increase in the strength of  $v(r_{ij})$  that would then contribute to an improved spectrum. The answer comes from comparing the values of  $J_i$  for  $F(R_{ij}) = 1$  (all  $J_i$  are unity) and for  $F(R_{ij})$  used here. For Eq. (5) with  $A_0 = 5.5$  the values of  $J_i$  for those  $i$  affecting these calculations are shown in Table I.

Thus, we conclude, good agreement between experimental and theoretical low-lying spectra is achieved in cases (5) and (6) without effectively increasing the strength of  $v(r_{ij})$ . Furthermore, we see that the  $J_i$  do not at all act in any approximate multiplicative manner.

Next, we concentrate on the observed spreading of the neutron strength as indicated by the spectroscopic factors. Table II summarizes the values of  $[(2J_f + 1)/(2J_i + 1)]S_{ij}$  obtained in the  $(d, p)$  and  $(d, {}^3\text{He})$  experiments.  $J_i$  and  $J_f$  represent the spins of the target and final nucleus, respectively. Tables III–V give the spectroscopic factors predicted by cases (1), (4), and (6), respectively, for the  $(d, p)$ ,  $(d, {}^3\text{He})$ , and a possible proton stripping reaction such as a  $({}^3\text{He}, d)$  experiment.

Two distinct groups of  $l_n = 2$  transfers were seen in the  $(d, p)$  experiments suggesting the  $|g_{9/2}^{-1}d_{5/2}\rangle$  strength was situated between 4 and 5 MeV and the  $|g_{9/2}^{-1}d_{3/2}\rangle$  strength was localized between 6 and 7 MeV. This is found to be true in all the calculations reported here. In spite of greater configuration mixing obtained with the surface interactions, Tables III–V indicate that the  $d_{5/2}$  and  $d_{3/2}$  neutron strengths remain well separated. In all the cases the total strength of the  $|g_{9/2}^{-1}d_{5/2}\rangle$  configuration below 5.1 MeV nearly exhausts the sum rule and only a small fraction of the  $|g_{9/2}^{-1}d_{3/2}\rangle$  total strength is seen in this region.

TABLE I. The Talmi integrals  $J_i$  for the center of mass part of the effective interaction given in Eq. (5) with  $A_0 = 5.5$ .

$i$	$J_i$
0	0.0001
1	0.0011
2	0.0061
3	0.0239
4	0.0735
5	0.1845
6	0.3923
7	0.7226
8	1.1746

TABLE II. Spectroscopic factors from the  $(d, p)$  and  $(d, {}^3\text{He})$  experiments leading to final states in  ${}^{88}\text{Sr}$ .

${}^{87}\text{Sr}(d, p){}^{88}\text{Sr}$				${}^{89}\text{Y}(d, {}^3\text{He}){}^{88}\text{Sr}$					
$J^\pi$	$l_n$	$E$	$\frac{2J_f + 1}{2J_i + 1} S_{ij}$		$J^\pi$	$l_n$	$E$	$\frac{2J_f + 1}{2J_i + 1} S_{ij}$	
			a	b				c	d
$2^+$	2	1.836	0.126		$2^+$	1,3	1.836	2.2	2.5
	2	4.033	0.279	0.35	$2^+$	1,3	3.220	1.6	3.3
	2	4.294	0.376	0.53	$1^+$	1	3.487	1.2	1.5
	2	4.408	0.875	1.18	$3^+$	3	3.635	2.2	3.3
	2	4.450	0.083	(~0.10)					
	2	4.514	1.08	1.31					
	2	4.633	0.564	0.68					
	2	4.744	0.805	0.14					
	0	4.876	0.230						
	2	5.094	1.04	1.33					

<sup>a</sup> See Ref. 19.

<sup>b</sup> See Ref. 20.

<sup>c</sup> See Ref. 26.

<sup>d</sup> Average of results from Ref. 25.

Closer examination of the  $(d, p)$  results show that the neutron strength is considerably spread out among the low-lying levels. Though the surface interactions achieve greater neutron strength spreading, all the calculations achieved less spreading than the experiments seem to indicate. Note that the  $(t, p)$  experiment of Ragaini and Knight<sup>27</sup> finds a  $0^+$  state at 3.151 MeV and another at 4.484 MeV which are not accommodated by our choice of model space. Furthermore, as many as six levels of  $2^+$  assignment have been seen below 5 MeV and our analysis allows for a total of only four  $2^+$  levels. These observations lead us to the conclusion that in order to achieve better agreement with experiment for the low-lying levels it is necessary to include higher configurations such as 1p-1h configurations above 7 MeV and 2p-2h configurations. The results for the lowest  $2^+$  state should not, however, be seriously effected by the 2p-2h contributions, since, by the  $(d, {}^3\text{He})$  and the  $(d, p)$  experiments all its strength has been accounted for. To a lesser degree this is true of the second  $2^+$  at 3.21 MeV which has 60% of its strength accounted for in these reactions. We conclude that the structure of all the  $2^+$  states but the lowest probably exhibit some 2p-2h admixtures.

Since the  $2^+$  state at 1.84 MeV has all its strength accounted for in the  $(d, p)$  and  $(d, {}^3\text{He})$  experiments (25 and 75%, respectively) it serves as a good test of the wave functions resulting from the various residual interactions. Cases (1)–(3) predicted about 15% of the state would be neutron  $|g_{9/2}^{-1}d_{5/2}\rangle$  configuration, whereas the surface interactions, cases (3)–(6) yielded between 25 and

TABLE III. Theoretical spectroscopic factors for  $(d,p)$ ,  $(d, {}^3\text{He})$ , and  $({}^3\text{He}, d)$  obtained in case (1). We show the contribution of the various orbitals to the total spectroscopic factor to facilitate comparison with the observed angular distributions as well.

Case (1), spectroscopic factors: $\frac{2J_f+1}{2J_i+1} S_{ij}$											
$J^\pi$	$E$	$s_{1/2}$	$(d,p) J_i = \frac{3}{2}$			$(d, {}^3\text{He}) J_i = \frac{1}{2}$			$({}^3\text{He}, d) J_i = \frac{3}{2}$		
			$d_{5/2}$	$d_{3/2}$	Total	$p_{3/2}$	$f_{5/2}$	Total	$p_{1/2}$	$g_{9/2}$	Total
2 <sup>+</sup>	2.61		0.093		0.093	1.282	0.749	2.03	0.641		0.641
2 <sup>+</sup>	3.26		0.021		0.021	1.087	1.266	2.35	0.544		0.544
3 <sup>-</sup>	3.45									1.534	1.534
1 <sup>+</sup>	3.54					1.381		1.381	0.691		0.691
3 <sup>+</sup>	3.72		0.010	0.001	0.011		3.444	3.444			
5 <sup>-</sup>	3.89									2.714	2.714
7 <sup>-</sup>	3.99										
4 <sup>-</sup>	4.10									2.036	2.036
4 <sup>+</sup>	4.11	0.032	0.864	0.004	0.900						
2 <sup>+</sup>	4.16		0.385		0.385	0.089	0.480	0.570	0.045		0.045
6 <sup>+</sup>	4.21		1.279	0.020	1.299						
3 <sup>+</sup>	4.25		0.679	0.009	0.688		0.055	0.055			
6 <sup>-</sup>	4.29									2.027	2.027
5 <sup>+</sup>	4.38	0.011	1.081	0.007	1.099						
3 <sup>-</sup>	4.39									0.098	0.098
2 <sup>-</sup>	4.43										
6 <sup>-</sup>	4.46									1.223	1.223
5 <sup>-</sup>	4.48									0.036	0.036
7 <sup>+</sup>	4.60		1.499		1.499						
4 <sup>-</sup>	4.71									0.085	0.085

30%. Table VI summarized the amplitudes of the main components of this state and indicates where the remaining strength lies. The experiments appear to support the surface interaction energy levels and wave functions for this state. Table VI also displays the results of Hughes<sup>32</sup> expressed in

this coupling scheme.

We calculated the  $B(E2)$  transitions for this state with and without effective charges. The values chosen for the effective charges were  $1.5e$  for the protons and  $0.5e$  for the neutrons. The neutron contributions were of the same sign as the proton

TABLE IV. Theoretical spectroscopic factors for  $(d,p)$ ,  $(d, {}^3\text{He})$ , and  $({}^3\text{He}, d)$  obtained in case (4). We show the contribution of the various orbitals to the total spectroscopic factor to facilitate comparison with the observed angular distributions as well.

Case (4), spectroscopic factors: $\frac{2J_f+1}{2J_i+1} S_{ij}$											
$J^\pi$	$E$	$s_{1/2}$	$(d,p) J_i = \frac{3}{2}$			$(d, {}^3\text{He}) J_i = \frac{1}{2}$			$({}^3\text{He}, d) J_i = \frac{3}{2}$		
			$d_{5/2}$	$d_{3/2}$	Total	$p_{3/2}$	$f_{5/2}$	Total	$p_{1/2}$	$g_{9/2}$	Total
2 <sup>+</sup>	2.05		0.137		0.137	0.408	1.405	1.81	0.204		0.204
3 <sup>-</sup>	3.03									1.066	1.066
2 <sup>+</sup>	3.38		0.071		0.071	1.995	0.115	2.11	0.998		0.998
3 <sup>+</sup>	3.62		0.121	0.017	0.138		2.78	2.78			
1 <sup>+</sup>	3.79					1.486		1.486	0.743		0.743
5 <sup>-</sup>	3.91									2.74	2.74
4 <sup>+</sup>	4.02	0.026	0.874	<0.001	0.900						
6 <sup>+</sup>	4.18		1.29	0.007	1.30						
4 <sup>-</sup>	4.28									1.567	1.567
2 <sup>-</sup>	4.35										
3 <sup>-</sup>	4.39									0.307	0.307
6 <sup>-</sup>	4.42									0.897	0.897
7 <sup>-</sup>	4.53										
5 <sup>+</sup>	4.65	0.158	0.933	0.007	1.098						
5 <sup>-</sup>	4.68									0.008	0.008
2 <sup>+</sup>	4.89		0.274		0.274	0.044	0.839	0.883	0.022		0.022
3 <sup>+</sup>	4.89		0.533	0.079	0.612		0.396	0.396			

TABLE V. Theoretical spectroscopic factors for  $(d, p)$ ,  $(d, {}^3\text{He})$ , and  $({}^3\text{He}, d)$  obtained in case (6). We show the contribution of the various orbitals to the total spectroscopic factor to facilitate comparison with the observed angular distributions as well.

Case (6), spectroscopic factors: $\frac{2J_f+1}{2J_i+1} S_{ij}$											
$J^\pi$	$E$	$s_{1/2}$	$(d, p) J_i = \frac{3}{2}$			$(d, {}^3\text{He}) J_i = \frac{1}{2}$			$({}^3\text{He}, d) J_i = \frac{3}{2}$		
			$d_{5/2}$	$d_{3/2}$	Total	$p_{3/2}$	$f_{5/2}$	Total	$p_{1/2}$	$g_{9/2}$	Total
$2^+$	1.90		0.159		0.159	1.343	0.360	1.703	0.671		0.671
$3^-$	2.98									1.076	1.076
$1^+$	3.44					1.418		1.418	0.709		0.709
$2^+$	3.71		0.011		0.011	0.318	2.101	2.420	0.159		0.159
$3^+$	3.86		0.049	0.001	0.050		3.236	3.236			
$5^-$	3.96									2.734	2.734
$4^+$	4.11	0.025	0.874	0.001	0.900						
$6^+$	4.26		1.291	0.007	1.298						
$4^-$	4.31									1.587	1.587
$2^-$	4.41										
$6^-$	4.43									0.832	0.832
$3^-$	4.48									0.239	0.239
$7^-$	4.50										
$5^-$	4.60									0.016	0.016
$5^+$	4.63	0.141	0.949	0.007	1.097						
$3^+$	4.78		0.609	0.041	0.650		0.250	0.250			
$2^+$	4.87		0.317		0.317	0.727	0.031	0.759	0.364		0.364
$4^-$	4.90									0.660	0.660
$6^-$	4.95									2.418	2.418

contributions and therefore enhanced the  $B(E2)$  transitions. The obtained  $B(E2)$  values using these effective charges are given in Table VII and compared with experiment as well as with other theoretical works. We note that even the calculation of Gillet *et al.*<sup>33</sup> using the RPA plus collective core admixture fails by a wide margin to reproduce the  $B(E2)$  with bare charges. In the light of this the results of Hughes would appear to be rather remarkable. However, his calculation distributes *all* the strength to proton orbitals, while other more realistic calculations distribute significant strength to the neutrons for this state.

The second  $2^+$  at 3.21 MeV is only weakly excited by the  $(d, p)$  experiment indicating it has little neutron 1p-1h contributions involving  $g_{9/2}$  hole states. All our calculations except the one with the SDI predict only 3–6% of 1p-1h neutron strength. The calculation with the surface  $\delta$  interaction yields about 15% of neutron 1p-1h configura-

tions.

As in the case of the second  $2^+$ , the first  $3^-$  at 2.74 MeV is only weakly excited in the  $(d, p)$  experiment. It was not seen at all in the  $(d, {}^3\text{He})$  experiment. These observations are consistent with our choice of space. The 1p-1h neutron states included in our space cannot couple to a  $J=3^-$  state. However, since the state has a direct transition from the capture state in  $(n, \gamma)$ , a small admixture of the  $|g_{9/2}^{-1}h_{11/2} J=3\rangle$  configuration may be present which our calculation would not account for. Cases (1)–(3) produced a relatively pure  $|p_{3/2}^{-1}g_{9/2} J=3\rangle$  proton state, whereas the surface interactions yielded a more complicated state, with a few configurations of considerable strength. The strength of the  $|p_{3/2}^{-1}g_{9/2} J=3\rangle$  configuration should be directly measurable in the suggested  $({}^3\text{He}, d)$  experiment. Cases (4)–(6) produced about a 35% neutron 1p-1h contribution nearly all of which was due to the  $|p_{1/2}^{-1}d_{5/2} J=3\rangle$  configura-

TABLE VI. Amplitudes of the main components of the first excited  $2^+$  state in  ${}^{88}\text{Sr}$ . For comparison the results of Hughes (Ref. 32) are also presented in this coupling scheme.

Ref.	$E$	$ p_{3/2}^{-1}p_{1/2}\rangle$	$ f_{5/2}^{-1}p_{1/2}\rangle$	Remaining str.
Hughes <sup>a</sup>	1.91	0.757	0.514	16% proton 2p-2h
Case (1)	2.61	0.716	0.547	19% neutron 1p-1h
Case (4)	2.05	0.404	0.750	27% neutron 1p-1h
Case (6)	1.90	0.733	0.380	32% neutron 1p-1h

<sup>a</sup> See Ref. 32.



TABLE VII. Comparison between experiment and theory for the  $B(E2)$  of the transition from the ground state to the first excited  $2^+$  state. The abbreviations are as follows: q.p. is for quasiparticle, TDA is for Tamm-Dancoff approximation, and RPA is for random phase approximation. For other details of the theoretical calculations see the appropriate references. When an author quotes only the ratio we do not extract an absolute  $B(E2)_{\text{th}}$  unless he also quotes the  $B(E2)_{\text{exp}}$  that he employed. The results in parentheses are obtained when the effective charges described in the text are employed.

Reference	Method or theory	$E$	$B(E2)$ ( $e^2\text{fm}^4$ )	$B(E2)_{\text{exp}}/B(E2)_{\text{th}}$
<i>Experiment</i>				
Peterson and Alster (Ref. 47)	$(e, e')$	1.83	990 $\pm$ 50	
<i>Theory</i>				
Gillet <i>et al.</i> (Ref. 33)	2 q.p. TDA	2.01	252	3.93
	2 q.p. RPA	1.99	273	3.63
	2 q.p. + core TDA	2.06	269	3.68
	2 q.p. + core RPA	1.99	300	3.30
Shastry (Ref. 31)	p-h shell model			4.65
Hughes (Ref. 32)	2 proton holes in $^{80}\text{Zr}$		395	2.5
This work	Case (1)	2.61	179 (588)	5.53 (1.68)
	Case (4)	2.05	151 (547)	6.59 (1.81)
	Case (6)	1.90	139 (532)	7.12 (1.86)

tion which could not be seen in the  $(d, p)$  experiment. Table VIII summarizes the main components of the calculated wave functions for this state. The  $B(E3)$  transitions are calculated with and without effective charges. We choose the same effective charge for the octupole transition as for the quadrupole case. Again, the neutron strength adds coherently with the protons and significantly improves the calculated result. The values obtained using effective charge are given in parentheses in Table IX and again we compare with experiment and other theoretical values. Note that, in this case, the extensions to the shell model by Gillet do improve agreement between theory and experiment with bare charges.

A  $1^+$  level near 3.5 MeV has been observed in the  $(d, ^3\text{He})$  (3.48),  $\beta$  decay (3.488),  $(p, p')$  (3.487), and  $(n, \gamma)$  (3.487) experiments. The  $(n, \gamma)$  results indicate it possesses a direct decay from the capture state. On the other hand it was not seen in

the  $(d, p)$  experiment. We compare this state with the low-lying  $1^+$  state found in our calculations. Cases (1), (2), and (3) produced a  $1^+$  at 3.54, 3.57, and 4.01 MeV, respectively. Cases (4), (5), and (6) yielded  $1^+$  levels at 3.79, 3.27, and 3.44 MeV, respectively. The configurations contributing to the  $1^+$  state are the  $|p_{3/2}^{-1}p_{1/2}\rangle$  and  $|g_{9/2}^{-1}g_{7/2}\rangle$  with the various calculations yielding about 5–10% of the latter. These wave functions are then consistent with all the experimental information.

All the calculations produced a  $3^+$  state between 3.6 and 3.9 MeV. The energy and spectroscopic factors indicate this calculated state agrees well with the 3.64 MeV strong stripping state with  $3^+$  assignment seen in the  $(d, ^3\text{He})$  work. This level is also observed in  $\beta$  decay at 3.635 MeV with a probable  $3^+$  assignment and in  $(n, \gamma)$  with a direct transition from the capture state. Cases (1)–(3) predict the  $3^+$  will be a nearly pure  $|f_{5/2}^{-1}p_{1/2}\rangle$  proton configuration, but the surface interactions

TABLE VIII. Amplitudes of the main components of the first excited  $3^-$  state in  $^{88}\text{Sr}$ . For comparison, the results of Shastry (Ref. 31) are presented.

Ref.	$E$	$ p_{3/2}^{-1}g_{9/2}\rangle$	$ f_{5/2}^{-1}g_{9/2}\rangle$	Remaining str.
Shastry <sup>a</sup>	2.76	0.958	0.043	8% other 1p-1h
Case (1)	3.45	0.936	0.012	12% neutron 1p-1h
Case (4)	3.03	0.780	-0.134	37% neutron 1p-1h
Case (6)	2.98	0.784	-0.127	37% neutron 1p-1h

<sup>a</sup> See Ref. 31.

TABLE IX. Comparison between experiment and theory for the  $B(E3)$  from the ground state to the first excited  $3^-$  state. For the abbreviations see the caption to Table VII. The results in parentheses are obtained when the effective charges described in the text are employed.

Reference	Method or theory	$E$	$B(E3)$ ( $e^2\text{fm}^6$ )	$B(E3)_{\text{exp}}/B(E3)_{\text{th}}$
<i>Experiment</i>				
Peterson and Alster (Ref. 47)	$(e, e')$	2.74	80 600 $\pm$ 3 000	
<i>Theory</i>				
Gillet <i>et al.</i> (Ref. 33)	2 q.p. TDA	3.29	13 330	6.05
	2 q.p. RPA	3.28	14 670	5.49
	2 q.p. + core TDA	2.83	25 080	3.21
	2 q.p. + core RPA	2.22	57 160	1.41
Picard <i>et al.</i> (Ref. 21)	2 q.p. + core RPA1	2.5		2.0
	2 q.p. + core RPA2	2.0		1.5
Shastry (Ref. 31)	p-h shell model			2.16
This work	Case (1)	3.45	9 281 (26 073)	8.68 (3.09)
	Case (4)	3.03	7 341 (23 718)	11.0 (3.40)
	Case (6)	2.98	7 359 (24 121)	11.0 (3.34)

predict the state has from 10 to 20%  $|g_{9/2}^{-1}d_{5/2}\rangle$ ,  $|g_{9/2}^{-1}d_{3/2}\rangle$ , and  $|g_{9/2}^{-1}g_{7/2}\rangle$  configurations. Thus, we see that although there is significantly more configuration mixing in the  $3^+$ , the available data are not sufficient to distinguish between the wave functions.

Above these states all our calculations yield some states that have not been discussed in previous theoretical studies. In particular at least one  $5^-$ ,  $6^-$ , and  $7^-$  are found between 3.5 and 4.5 MeV. These could coincide with the levels observed in the recent  $^{86}\text{Kr}(\alpha, 2n)^{88}\text{Sr}$  experiment<sup>29</sup> at 3585, 4020, and 4368 MeV with probable assignments  $(5)^-$ ,  $(6)^-$ , and  $(7)^-$ , respectively.

In addition we find a  $4^+$ ,  $5^+$ ,  $6^+$ , and  $7^+$  between 4 and 5.5 MeV (though not always listed in Tables III-V which could account for some of the strong  $(d, p)$  strength seen experimentally. Conclusive experimental evidence for these states is lacking, however.

## VII. SUMMARY

We have seen that, by using surface restricted residual interactions in a shell model calculation of the spectrum of  $^{88}\text{Sr}$ , good results can be achieved.

Our calculations indicate that finite-range re-

sidual interactions restricted to the nuclear surface can improve the results over those obtained when the same residual interactions are allowed to act throughout the nuclear volume. The interactions used in cases (5) and (6) fall into the general category of density dependent effective interactions. We mentioned already that Sharp and Zamick as well as Ring and Speth have used density dependent forces in order to calculate the residual particle-hole interactions. In their calculation the interaction is of finite range in the center of mass coordinate  $R_{ij}$  and zero range in the relative coordinate  $r_{ij}$ . In our calculation, however, the interaction is of zero range in  $R_{ij}$  but the particles are allowed to interact at finite range once they are at the nuclear surface. A generalization of both approaches is of course an interaction which is of finite range in both  $r$  and  $R$ . Although the  $^{88}\text{Sr}$  nucleus served more as a test case for the interactions we introduced, we were able to obtain interesting information concerning the structure of this nucleus.

We would like to thank Professor D. Alan Bromley for his hospitality at Yale University during the initial phases of this work. Suggestions from C. W. Wong in the early states of this work are acknowledged.

<sup>†</sup> Work supported by the U.S. Energy Research and Development Administration.

\*Present address.

‡Present address.

<sup>1</sup>H. A. Bethe, invited talk, 1967 Annual Meeting of the American Physical Society, New York (unpublished).

<sup>2</sup>S. A. Moszkowski, *Phys. Rev. C* **2**, 402 (1970).

<sup>3</sup>R. W. Sharp and L. Zamick, *Nucl. Phys. A* **208**, 130 (1973).

- <sup>4</sup>P. Ring and J. Speth, Nucl. Phys. A235, 315 (1974).
- <sup>5</sup>T. H. R. Skyrme, Phil. Mag. 1, 1043 (1956); Nucl. Phys. 9, 615 (1959).
- <sup>6</sup>K. A. Brueckner, J. L. Gammel, and H. Weitzner, Phys. Rev. 110, 431 (1958); K. A. Brueckner, A. M. Lockett, and M. Rotenberg, *ibid.* 121, 255 (1961); N. E. Reid, M. K. Banerjee, and G. J. Stephenson, Jr., Phys. Rev. C 5, 41 (1972).
- <sup>7</sup>D. W. L. Sprung and P. K. Banerjee, Nucl. Phys. A168, 273 (1971); G. Fái and J. Németh, *ibid.* A208, 463 (1973); J. Németh and G. Ripka, *ibid.* A194, 329 (1972).
- <sup>8</sup>C. W. Wong, Nucl. Phys. A91, 399 (1967); A. M. Green, Phys. Lett. 24B, 384 (1967); H. S. Köhler, Nucl. Phys. A91, 593 (1967).
- <sup>9</sup>R. Rajaraman and H. A. Bethe, Rev. Mod. Phys. 39, 745 (1967); H. A. Bethe, Ann. Rev. Nucl. Sci. 21, 93 (1971).
- <sup>10</sup>A. B. Migdal, *Theory of Finite Fermi Systems and Applications to Atomic Nuclei* (Interscience, New York, 1967).
- <sup>11</sup>V. R. Pandharipande, Nucl. Phys. A115, 516 (1968); Phys. Lett. 29B, 1 (1969).
- <sup>12</sup>G. E. Brown, Rev. Mod. Phys. 43, 1 (1971).
- <sup>13</sup>J. W. Negele, Phys. Rev. C 1, 1260 (1970); H. S. Köhler, Nucl. Phys. A170, 88 (1971); S. A. Coon and H. S. Köhler, *ibid.* A231, 95 (1974).
- <sup>14</sup>D. M. Brink and D. Vautherin, Phys. Lett. 32B, 149 (1970); D. Vautherin and D. M. Brink, Phys. Rev. C 5, 626 (1972).
- <sup>15</sup>K. R. Lassey and A. B. Volkov, Phys. Lett. 36B, 4 (1971).
- <sup>16</sup>J. W. Negele and D. Vautherin, Phys. Rev. C 5, 1472 (1972); J. W. Negele and D. Vautherin, *ibid.* 11, 1031 (1975).
- <sup>17</sup>J. W. Ehlers and S. A. Moszkowski, Phys. Rev. C 6, 217 (1972).
- <sup>18</sup>J. W. Negele, Proceedings of the Tucson Meeting on Effective Interactions and Operators, June 1975, Lecture Notes in Physics, (Springer-Verlag, Heidelberg, 1975), Vol. 40.
- <sup>19</sup>E. R. Cosman and D. C. Slater, Phys. Rev. 172, 1126 (1968).
- <sup>20</sup>K. K. Seth, K. A. Buzard, J. Picard and G. Bassani, Phys. Rev. C 10, 1928 (1974); K. K. Seth, K. A. Buzard, J. Picard, and G. Bassani, *ibid.* 11, 2087 (1975).
- <sup>21</sup>J. Picard, O. Beer, A. El Behay, P. Lopato, Y. Terrien, G. Vallois, and R. Schaeffer, Nucl. Phys. A128, 481 (1969).
- <sup>22</sup>M. M. Stautberg, J. J. Kraushaar, and B. W. Ridley, Phys. Rev. 157, 977 (1967).
- <sup>23</sup>F. E. Cecil, R. P. Chestnut, and R. L. McGrath, Phys. Rev. C 10, 2425 (1974).
- <sup>24</sup>J. L. Irigaray, G. Y. Petit, P. Carlos, B. Maier, R. Samama, and H. Nifenecker, Nucl. Phys. A113, 134 (1968); G. A. Bartholomew, A. Doveika, K. M. Eastwood, S. Monaro, L. V. Groshev, A. M. Demidov, V. I. Pelekhov, and L. L. Sokolovskii, Nucl. Data A3, 367 (1967); H. Schmidt, W. Michaelis, C. Weitkamp, and G. Markus, Z. Phys. 194, 373 (1966); H. Lycklama and T. J. Kennett, Nucl. Phys. A139, 625 (1969).
- <sup>25</sup>J. F. Harrison and J. C. Hiebert, Nucl. Phys. A185, 385 (1972).
- <sup>26</sup>C. D. Kavaloski, J. S. Lilley, D. C. Shreve, and N. Stein, Phys. Rev. 161, 1107 (1967).
- <sup>27</sup>R. C. Ragaini and J. D. Knight, Nucl. Phys. A125, 97 (1969); H. Lycklama, N. P. Archer, and T. J. Kennett, Can. J. Phys. 47, 393 (1969).
- <sup>28</sup>R. L. Bunting, W. L. Talbert, Jr., J. R. McConnell, and R. A. Meyer, this issue, Phys. Rev. C 13, 1577 (1976).
- <sup>29</sup>S. E. Arnell, A. Nilsson, and O. Stankiewicz, Nucl. Phys. A241, 109 (1975).
- <sup>30</sup>S. Shastri and A. K. Saha, Nucl. Phys. 85, 393 (1966); A97, 567 (1967).
- <sup>31</sup>S. Shastri, Nucl. Phys. A142, 12 (1970).
- <sup>32</sup>T. A. Hughes, Phys. Rev. 181, 1586 (1969).
- <sup>33</sup>V. Gillet, B. Giraud, J. Picard, and M. Rho, Phys. Lett. 27B, 483 (1968).
- <sup>34</sup>S. Shastri, Phys. Lett. 28B, 85 (1968).
- <sup>35</sup>F. E. Cecil, T. T. S. Kuo, and S. F. Tsai, Phys. Lett. 45B, 217 (1973).
- <sup>36</sup>F. Everling, L. A. König, J. H. E. Mattauch, and A. H. Wapstra, Nucl. Phys. 18, 529 (1960).
- <sup>37</sup>L. Rosenfeld, *Nuclear Forces* (North-Holland, Amsterdam, 1948), p. 233.
- <sup>38</sup>A. Kallio and K. Kolltveit, Nucl. Phys. 53, 87 (1964).
- <sup>39</sup>B. L. Scott and S. A. Moszkowski, Nucl. Phys. 29, 665 (1962); S. A. Moszkowski and B. L. Scott, Ann. Phys. (N.Y.) 11, 65 (1960).
- <sup>40</sup>I. M. Green and S. A. Moszkowski, Phys. Rev. 139, B790 (1965).
- <sup>41</sup>R. Arvieu and S. A. Moszkowski, Phys. Rev. 145, 830 (1966); A. Plastino, R. Arvieu, and S. A. Moszkowski, *ibid.* 145, 837 (1966); J. Letourneux and J. M. Eisenberg, Nucl. Phys. 85, 119 (1966).
- <sup>42</sup>B. H. Wildenthal, J. B. McGrory, E. C. Halbert, and P. W. M. Glaudemans, Phys. Lett. 27B, 611 (1968).
- <sup>43</sup>C. W. Wong and S. A. Moszkowski, (unpublished).
- <sup>44</sup>B. H. Brandow, Rev. Mod. Phys. 39, 771 (1967).
- <sup>45</sup>I. Talmi, Helv. Phys. Acta 25, 185 (1952).
- <sup>46</sup>T. A. Brody and M. Moshinsky, *Tables of Transformation Brackets* (Monografias del Instituto de Fisica, Mexico, 1960).
- <sup>47</sup>G. A. Peterson and J. Alster, Phys. Rev. 166, 1136 (1968).